Dynamical Reduction of the Dimensionality of Exchange Interactions and the "Spin-Liquid" Phase of κ-(BEDT-TTF)$_2$X

B. J. Powell,[1,*] E. P. Kenny,[1] and J. Merino[2]

[1]*School of Mathematics and Physics, The University of Queensland, Brisbane, Queensland 4072, Australia*
[2]*Departamento de Física Teórica de la Materia Condensada, Condensed Matter Physics Center (IFIMAC)
and Instituto Nicolás Cabrera, Universidad Autónoma de Madrid, Madrid 28049, Spain*

We show that the anisotropy of the effective spin model for the dimer Mott insulator phase of κ-(BEDT-TTF)$_2$X salts is dramatically different from that of the underlying tight-binding model. Intradimer quantum interference results in a model of coupled spin chains, where frustrated interchain interactions suppress long-range magnetic order. Thus, we argue, the "spin liquid" phase observed in some of these materials is a remnant of the Tomonaga-Luttinger physics of a single chain. This is consistent with previous experiments and resolves some outstanding puzzles.

Layered organic charge transfer salts show a wide range of exotic physics due to strong electronic correlations and geometrical frustration [1]. This includes unconventional superconductivity, incoherent metallic transport, multiferroicity, and antiferromagnetism. However, the putative spin liquid states in κ-(BEDT-TTF)$_2$Cu$_2$(CN)$_3$ [2], κ-(BEDT-TTF)$_2$Ag$_2$(CN)$_3$ [3] (henceforth, CuCN and AgCN, respectively), and β'-EtMe$_3$Sb[Pd(dmit)$_2$]$_2$ [4] are, perhaps, the least understood of these.

CuCN is usually discussed in terms of the nearly triangular Heisenberg model [1,5]. Here, we demonstrate that the theoretical arguments that lead to this model are fallacious. They fail to account for quantum interference within the (BEDT-TTF)$_2$ dimer. We derive the correct low-energy model including these effects and show that it leads to an anisotropic triangular lattice in the quasi-one-dimensional (Q1D) regime, $J_1 > J_2$, Fig. 1(c). Thus, the spin model for the Mott dimer insulating phases of the organic charge transfer salts are remarkably similar to that describing Cs$_2$CuBr$_4$ and Cs$_2$CuCl$_4$ [6], where deconfined spinons have been observed [5,7]. Our results provide natural explanations for several previously puzzling experiments on the organics.

Electronic structure calculations demonstrate that a single molecular orbital contributes to the low-energy process in the κ-(BEDT-TTF)$_2$X salts [1,8–10], and that the band structure is described by the tight-binding "monomer model" sketched in Fig. 1(a) at three quarters filling. This model is dimerized: $t_{b1} \gg t_{b2}, t_p, t_q$. At ambient pressure CuCN, AgCN, and κ-(BEDT-TTF)$_2$Cu[N(CN)$_2$]Cl (henceforth, κ-Cl) display a Mott dimer insulating phase, where excitations away from exactly one hole per dimer are bound [1].

Electronic correlations arise from the Coulombic repulsion between two holes on the same monomer, U_m, or dimer, V_m. Thus, the effective Hamiltonian for the ith dimer is $\mathcal{H}_{b1}^{(i)} = -t_{b1}\sum_\sigma(\hat{c}_{i1\sigma}^\dagger\hat{c}_{i2\sigma} + \text{H.c.}) + U_m\sum_\mu\hat{n}_{i\mu\uparrow}\hat{n}_{i\mu\downarrow} + V_m\hat{n}_{i1}\hat{n}_{i2}$, where $\hat{c}_{i\mu\sigma}^{(\dagger)}$ annihilates (creates) an electron with spin σ on the μth monomer of the ith dimer, $\hat{n}_{i\mu\sigma} = \hat{c}_{i\mu\sigma}^\dagger\hat{c}_{i\mu\sigma}$, and $\hat{n}_{i\mu} = \sum_\sigma\hat{n}_{i\mu\sigma}$. Other Coulomb matrix elements can also be included, but do not qualitatively change our results and are neglected below. The hopping between dimers is given by $\mathcal{H}_1 = -t_{b2}\sum_{\langle i,j\rangle\sigma}(\hat{T}_{21} + \hat{T}_{21}^\dagger)$ and $\mathcal{H}_2 = \sum_{[i,j]\sigma}[-t_p(\hat{T}_{21} + \hat{T}_{21}^\dagger) - t_q(\hat{T}_{22} + \hat{T}_{22}^\dagger)]$, where $\hat{T}_{\nu\mu} = \hat{c}_{i\nu\sigma}^\dagger\hat{c}_{j\mu\sigma}$, $\langle i,j\rangle$ implies a pair of dimers equivalent to tetramer 1 [Fig. 1(a)], and $[i,j]$ implies a pair of dimers such as tetramer 2.

Kino and Fukuyama (KF) showed that for large enough U_m an insulating phase emerges [8]. They argued that this could be understood as a dimer Mott insulator: if one integrates out the bonding combination of molecular orbitals, this leaves an effective half-filled model containing only the antibonding combination of molecular orbitals,
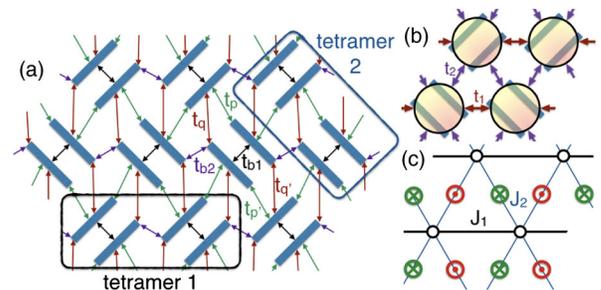

FIG. 1. Models of organic charge transfer salts: (a) Hopping integrals between monomers (bars). To an excellent approximation $t_q = t_{q'}$ and $t_p = t_{p'}$ [10]. (b) The dimer model. (c) Heisenberg model in the dimer Mott insulator phase, the staggered interlayer component of DM interaction is also indicated—we adopt the convention that the leftmost spin appears first in the DM interaction, $\boldsymbol{D}_{ij} \cdot \boldsymbol{S}_i \times \boldsymbol{S}_j$.

$a_{i\sigma}^\dagger = (1/\sqrt{2})(c_{i1\sigma}^\dagger - c_{i2\sigma}^\dagger)$. The "dimer model" is $\mathcal{H}_d = -t_1\sum_{\langle i,j\rangle\sigma}(\hat{a}_{i\sigma}^\dagger\hat{a}_{j\sigma}+\text{H.c.}) - t_2\sum_{[i,j]\sigma}(\hat{a}_{i\sigma}^\dagger\hat{a}_{j\sigma}+\text{H.c.}) + U_d\sum_i\hat{a}_{i\uparrow}^\dagger\hat{a}_{i\uparrow}\hat{a}_{i\downarrow}^\dagger\hat{a}_{i\downarrow}$, Fig. 1(b), where, for $V_m = 0$, $t_1/t_{b2} = t_2/(t_p + t_q) = \sqrt{2}(\cos\theta - \sin\theta)/4$, and $\tan\theta = (U_m/4t_{b1}) - \sqrt{1 + (U_m/4t_{b1})^2}$ [9]. KF estimated the effective interaction between two holes on the same dimer as $U_d = E_0(0) + E_0(2) - 2E_0(1) = 2t_{b1} + (U_m/2)[1 - \sqrt{1 + (4t_{b1}/U_m)}] \simeq 2t_{b1}$ for $U_m \gg 4t_{b1}$, where $E_0(N)$ is the ground state of the dimer with N holes. The $V_m \neq 0$ case is discussed in [11].

In the Mott dimer phase, KF's dimer model reduces to a Heisenberg model, Fig. 1(c)

$$\mathcal{H}_H = J_1\sum_{\langle i,j\rangle\sigma}\hat{\mathbf{S}}_i\cdot\hat{\mathbf{S}}_j + J_2\sum_{[i,j]\sigma}\hat{\mathbf{S}}_i\cdot\hat{\mathbf{S}}_j, \qquad (1)$$

where $\hat{\mathbf{S}}_i$ is the spin operator on the ith dimer, and in the dimer model $J_1 = 4t_1^2/U_d$ and $J_2 = 4t_2^2/U_d$.

Two decades of research have been based on these ideas. Thus, it is surprising that no one appears to have asked whether the same parameters for the Heisenberg model, Eq. (1), are found from both the monomer and dimer models. We do. The answer is no.

To calculate J_1, we perform a canonical transformation [12–14] taking $\mathcal{H}_0 = \sum_i\mathcal{H}_{b1}^{(i)}$ as our unperturbed Hamiltonian with the perturbation given by $\mathcal{H}_1$. We retain terms $O(t_{b2}^2)$ yielding the interaction described by the first term in Eq. (1).

The monomer model yields a larger J_1 than the dimer model, Fig. 2. This can be straightforwardly understood. The dimer with two electrons admits several low-lying excited states that allow for additional superexchange pathways, these are omitted from the dimer model. The exact energy differences between the lowest energy singlets and triplets for tetramer 1 [Figs. 1(a), 2] are in excellent agreement with the perturbative treatment of the monomer model but are very different from the J_1 calculated from the dimer model.

J_2 is calculated from the analogous treatment of the perturbation $\mathcal{H}_2$. Here, the predictions of the monomer model are strikingly different from the dimer model. J_2 is very rapidly suppressed by U_m in the monomer model, indeed, J_2 becomes ferromagnetic (< 0) for only moderate U_m at $V_m = 0$, Fig. 2. Again, a comparison with the exact low-energy states of tetramer 2 [Figs. 1(a), 2] demonstrates excellent agreement with the monomer model and profound differences from the dimer model. In the monomer model, J_2 remains finite and negative whereas $J_1 \to 0$ as $U_m \to \infty$.

Why is J_2 so different from J_1? The essential difference is that there are two hopping pathways in $\mathcal{H}_2$ and only one in $\mathcal{H}_1$. This allows destructive interference between the different exchange pathways that contribute to J_2, which are necessarily absent in the calculation of J_1. Furthermore, processes with amplitudes $\propto t_p t_q$ can take place without incurring an energetic penalty $\propto U_m$, Fig. 3. Thus, such processes remain active even as $U_m \to \infty$. Processes $\propto t_p t_q$ can favor ferromagnetic interactions. To understand this, it is helpful to consider two limiting cases.

(i) Molecular limit: $(U_m - V_m)/t_{b1} \to \infty$. A detailed understanding can be gained from considering the matrix elements

$$M_1 = \sum_n \frac{\langle\uparrow_i\downarrow_j|\hat{T}_{21}^\dagger|\Psi_n\rangle\langle\Psi_n|\hat{T}_{21}|\downarrow_i\uparrow_j\rangle}{2E_0(1) - \varepsilon_n}$$
$$= \frac{1}{16t_{b1}}((\langle S_i| - \langle T_i|)(|S_i\rangle + |T_i\rangle)) = 0, \qquad (2)$$

$$M_2 = \sum_n \frac{\langle\uparrow_i\downarrow_j|\hat{T}_{21}^\dagger|\Psi_n\rangle\langle\Psi_n|\hat{T}_{22}|\downarrow_i\uparrow_j\rangle}{2E_0(1) - \varepsilon_n}$$
$$= -\frac{1}{16t_{b1}}((\langle S_i| - \langle T_i|)(|S_i\rangle - |T_i\rangle)) = -\frac{1}{8t_{b1}}, \qquad (3)$$

where $|\sigma_i\rangle = (1/\sqrt{2})\hat{c}_{i1\sigma}^\dagger\hat{c}_{i2\sigma}^\dagger(\hat{c}_{i1\bar{\sigma}}^\dagger + \hat{c}_{i2\bar{\sigma}}^\dagger)|0\rangle$, $|S_i\rangle = (1/\sqrt{2})(\hat{c}_{i1\uparrow}^\dagger\hat{c}_{i2\downarrow}^\dagger - \hat{c}_{i1\downarrow}^\dagger\hat{c}_{i2\uparrow}^\dagger)|0\rangle$, $|T_i\rangle = (1/\sqrt{2})(\hat{c}_{i1\uparrow}^\dagger\hat{c}_{i2\downarrow}^\dagger + \hat{c}_{i1\downarrow}^\dagger\hat{c}_{i2\uparrow}^\dagger)|0\rangle$, and $(\mathcal{H}_{b1}^{(i)} + \mathcal{H}_{b1}^{(j)})|\Psi_n\rangle = \varepsilon_n|\Psi_n\rangle$. $|S_i\rangle$ and $|T_i\rangle$ become degenerate as $(U_m - V_m)/t_{b1} \to \infty$. In the
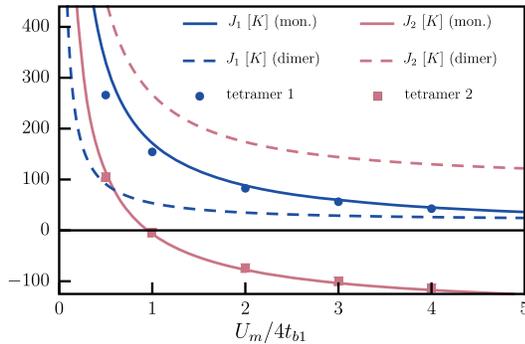

FIG. 2. Superexchange from perturbation theory for the monomer (solid lines) and dimer (dashed lines) models compared with the exact singlet-triplet splitting of the tetramers marked in Fig. 1(a) (dots and squares). Tight-binding parameters as calculated from first principles for κ-Cl and $V_m = 0$.
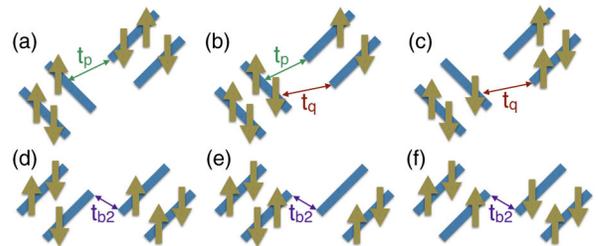

FIG. 3. Classical sketches of exchange process. (a)–(c) An exchange pathway that remains finite as $(U_m - V_m)/t_{b1} \to \infty$ contributing $\propto t_p t_q/t_{b1}$ to J_2. (d)–(f) An exchange pathway that vanishes as $U_m \to \infty$, contributing $\propto |t_{b2}|^2/U_m$ to J_1 for $U_m - V_m \gg t_{b1}$.

effective Heisenberg model, $J_1 = 2t_{b1}^2 M_1 + \cdots$ and $J_2 = 2t_p t_q M_2 + 2t_p^2 M_1 + \cdots$, where the ellipses include other terms at the same order, discussed below.

M_1 vanishes because the intermediate singlet and triplet excited states interfere destructively, whereas M_2 remains finite because the interference is constructive. All other contributions to J_1 vanish due to similar interference effects, thus, $J_1 = 0$. In contrast, the dimer model predicts that $J_1 \propto t_{b2}^2/t_{b1}$ in this limit. All terms in J_2 proportional to t_p^2 and t_q^2 also vanish by the same arguments. Including all terms at this order yields $J_2 = -t_p t_q/2t_{b1}$.

(ii) In the $U_m = V_m$ limit, the Hartree-Fock approximation becomes exact. This makes it straightforward to calculate the effective Heisenberg interaction, J_{gen}, for the more general perturbation $\mathcal{H}_{\text{gen}} = -\sum_{ij\mu\nu\sigma}(t_{\mu\nu}\hat{T}_{\mu\nu} + \text{H.c.})$. One finds that $J_{\text{gen}} = 2(t_{11} - t_{12} - t_{21} + t_{22})^2/U_m$. Thus, $J_1 = 2t_{b1}^2/U_m$ and $J_2 = 2(t_p - t_q)^2/U_m$. In this limit, the interference is a single particle phenomenon arising from the different phases of the two sites in the antibonding orbital. Thus, here, the details of the interference are quite different from the molecular limit. Nevertheless, one again finds that in the monomer model interference effects significantly suppress J_2 relative to expectations of the dimer model, where $J_2 \propto (t_p + t_q)^2$.

$J_2 > 0$ for all $U_m = V_m$. More generally, increasing V_m suppresses ferromagnetic exchange and eventually drives it antiferromagnetic, Fig. 4. Large ferromagnetic J_2 is inconsistent with experiment. This suggests that V_m/U_m is reasonably large, consistent with first principles estimates [11,15].

To consider specific materials, we take the hopping integrals from previous first principles calculations [10]. For reasonable parameters, the monomer model yields $J_2 < J_1$ in marked contrast to the dimer model, which gives $J_2 > J_1$, Fig. 4. We will describe this as dynamical
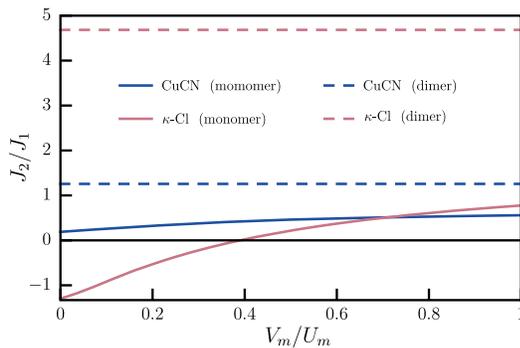

FIG. 4. Comparison of dimer (dashed lines) and monomer (solid lines) models for CuCN and κ-Cl (hopping integrals from [10] and $U_m = 12t_{b1}$). The dimer approximation predicts lattices between the square ($J_2/J_1 \to \infty$) and triangular ($J_2/J_1 = 1$) limits, whereas the monomer model gives lattices in the quasi-1D regime ($|J_2/J_1| < 1$) for reasonable parameters (say, $1/3 \lesssim V_m/U_m \lesssim 2/3$).

dimensionality reduction (DDR). Below, we will see that DDR, and the frustration inherent in the system, leads to a natural interpretation of the spin liquid phase in terms of coupled chains. Another important difference from the predictions of the dimer model is that the values of the interactions, U_m and V_m, are vital for determining the parameters of the Heisenberg model. These are not well known at present and may differ between materials, but the best estimates suggest that $U_m \gg t_{b1}$ and $V_m \lesssim U_m$ [11,15–17].

The similarities between the hopping integrals in the BEDT-TTF and Pd(dmit)$_2$ salts suggest that similar physics is at play in the latter. Again, the effective Heisenberg model is given by Eq. (1), and there are two significant interdimer hopping pathways that contribute to J_2, but a single pathway dominates J_1 [18].

In the 1D limit ($J_2 \to 0$), a paramagnetic Tomonaga-Luttinger liquid (TLL) is expected at low temperatures. Equation (1) with $J_1 > J_2 > 0$ received extensive attention [19–32] following the observation of a strong inelastic continuum, consistent with deconfined spinons, in neutron scattering experiments on Cs$_2$CuCl$_4$ [7], where $J_2 \simeq 0.34J_1$ [6]. Cs$_2$CuCl$_4$ displays spiral order at low temperatures. Nevertheless, the observed inelastic continuum is quantitatively reproduced by theories based on disjunctive TLLs [19].

Classically, model (1) has spiral order in the chain limit [20]. Quantum fluctuations enhance the one dimensionality of this state [20–27]. Indeed, Starykh et al. argued that the model is Q1D for $J_2 < 0.7J_1$ [21]. Numerical studies are particularly challenging because of the incommensurate wave vector that characterizes the spiral phase [26,27], and several other ground states are found to be energetically competitive [25–31].

However, this question may be academic: theory suggests that small interactions decide which competing phase is realized [21,33], as one expects on general grounds in frustrated systems. Series expansions [26] find that, if the magnetization does not vanish as $J_2 \to 0$, then it becomes small extremely rapidly, consistent with the Néel temperature, $T_N \sim \exp[-(J_1/J_2)^2]$, predicted from treating the intrachain dynamics via TLL theory and the interchain coupling via the random phase approximation (TL + RPA) [32].

Therefore, our prediction that $J_1 > J_2$ naturally explains the absence of long-range magnetic order in CuCN and AgCN. Namely, that the Q1D limit survives even for relatively large $J_2/J_1 < 1$, and thus, the spin liquid is a remnant of the TLL found in an isolated chain. Even if the materials order eventually, the exponential suppression of T_N can easily move this orders of magnitude below the lowest temperatures studied (10s of mK). Why then is κ-Cl antiferromagnetic? Two perturbations are formally relevant [21]: interlayer exchange, J_z; and the staggered interlayer component of the interchain Dzyaloshinskii-Moriya (DM)
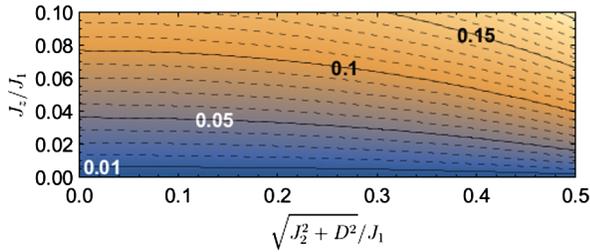
FIG. 5.   Calculated Néel temperature, T_N/J_1, for the Heisenberg model with interchain coupling treated at the RPA level. For reasonable parameters, a critical temperature ~20 K can be realized (cf. Fig. 2), as observed in κ-Cl.

interaction, D, cf. Fig. 1(c) [34–38] (an inversion center precludes DM coupling within the chains).

In the TL + RPA theory [32], the dynamic susceptibility is given by $\chi_{3D}^{+-}(\omega, \boldsymbol{k}) = \chi_{1D}^{+-}(\omega, k_x)/[1 - \tilde{J}(\boldsymbol{k})\chi_{1D}^{+-}(\omega, k_x)]$, where $\chi_{1D}^{+-}(\omega, k_x)$ is the susceptibility of a single chain perpendicular to D and the Fourier transform [39] of the interchain interactions is $\tilde{J}(\boldsymbol{k}) = -J_z \cos k_z \pm \sqrt{J_2^2 + D^2}[\cos(k_y/2) + \cos(k_x - k_y/2)]$. T_N is the highest temperature with a zero-frequency pole in $\chi_{3D}^{+-}(\omega, \boldsymbol{k})$. This is straightforwardly calculated as described in [32]. The solutions, Fig. 5, clearly indicate that, for reasonable parameters, it is possible to achieve $T_N/J_1 \sim 0.1$–0.2, consistent with observed critical temperature (~20 K) in κ-Cl, given our calculation of J_1, Fig. 2. Furthermore, J_z, which is unfrustrated, affects T_N far more strongly than D or J_2, suggesting this could be the essential difference between κ-Cl and CuCN. This could be tested by applying uniaxial strain perpendicular to the layers, which one would expect to increase J_z. This should increase T_N in κ-Cl and perhaps even drive CuCN or AgCN antiferromagnetic for sufficiently large strains, if the Mott transition does not intervene. Two intermonomer hopping integrals are relevant to interlayer hopping [40], so the interference effects that suppress J_2 also affect J_z. Thus, different materials may have radically different J_z.

It is important to ask how the DDR picture of the dimer Mott insulating organics compares with experiment.

Heat capacity varies linearly with temperature in a TLL [41] as observed in CuCN [42]. Thermal conductivity of CuCN does not reveal a term that varies linearly with temperature [43]. It has been widely assumed, on the basis of Q2D theories, that this is inconsistent with the heat capacity measurement. However, in a weakly disordered spin chain, the magnetic contribution to the thermal conductivity $\kappa_{\mathrm{mag}} \propto T^2$ [44], which is consistent with the measurements of CuCN, provided the magnetic contribution dominates the low temperature behavior [43]. One also expects a dip in κ_{mag} at $g\mu_B B \sim 4k_B T$ [44], which is also observed [45].

At low-frequencies, one expects a power-law in the optical conductivity of a TLL [41]. This is observed in both CuCN [46] and AgCN [47].

The bulk susceptibility of CuCN shows a broad maximum around ~70 K [2]. This can be fit reasonably well by high temperature series expansions for the isotropic triangular lattice [2,48]. However, for 1D chains, one also expects a broad maximum at $T = 0.64J$ [49], which would lead to the estimate $J_1 \sim 100$ K in CuCN.

The nuclear magnetic resonance (NMR) relaxation rate, $1/T_1$, in κ-Cl is well understood in terms of the incipient magnetic order [50,51]. In contrast, $1/T_1$ in CuCN is a long-standing problem [52–61]. $1/T_1$ in CuCN decreases as the temperature is lowered until a minimum is reached at ~6 K. A broad peak is then observed around 1 K. In spin chains, one expects a minimum in $1/T_1$ at $T \sim J_1/10$ concomitant with the crossover to a TLL [62]. There are no calculations, to date, describing $1/T_1$ in the presence of interchain interaction at temperatures above the TLL regime. Therefore, the only available comparison is with experimental results for Cs_2CuCl_4 [63]. Note that J_2/J_1 and the DM interaction are similar, but not identical, in the two materials, so the analogy is imperfect. However, one does not expect charge fluctuations to be especially important in the organics as no dramatic changes are observed under pressure until the first order metal-insulator transition. In Cs_2CuCl_4, one observes a broad peak around ~2.5 K, associated with the emergence of short-range order (SRO) [63,64], that is strongly reminiscent of the peak at ~1 K in CuCN. Microscopically, this SRO may be associated with the binding of spinons into triplons [5,19] driving a dimensional crossover and cutting off the logarithmic divergence in $1/T_1$ expected in a TLL.

Therefore, a natural explanation of $1/T_1$ in CuCN is that one sees a high temperature regime, a crossover to a TLL regime at $T \sim 6$ K, and the emergence of SRO/triplons at $T \sim 1$ K. These crossovers could also be responsible for the anomalies observed at the same characteristic temperatures in many other experiments [42,43,65–67]. A clear prediction of this interpretation is that the emergence of SRO should lead to the broadening of NMR spectra as the temperature is lowered [63]. This is, indeed, observed in ^{13}C NMR in CuCN; an observation that has eluded explanation in Q2D theories [68].

Antal *et al.* recently concluded that electron spin resonance (ESR) "in κ-Cl resembles the ESR in 1D Heisenberg chains with a Dzyaloshinskii-Moriya interaction" [37] just as our calculations suggest. Therefore, our prediction that the spin correlations in the insulating state are Q1D is consistent with many experiments.

Metallic organics display coherent in-plane electronic transport at low temperatures. DDR applies only to the spin correlations and so is not inconsistent with this. However, charge transport becomes incoherent above 20–40 K [69,70]. This suggests that the coherent interference processes, responsible for DDR, may be washed out when the temperature is raised. This would imply a strong temperature dependence in J_2/J_1 and lead to a dimensional

crossover at a much lower temperature scale than one would expect from the low temperature J_2/J_1.

J_2 favors $d_{x^2-y^2}$ superconductivity (taking the x and y axes to lie along the J_2 bonds), whereas J_1 favors $s + d_{xy}$ pairing [22,71]. Experimentally, the pairing symmetry in the organics remains controversial, but our results appear to favor $s + d_{xy}$ superconductivity, perhaps with accidental nodes.

Cs_2CuCl_4 displays a rich phase diagram as the strength and orientation of the magnetic field is varied [21,63,64]. Therefore, a more complete mapping of the physics of the organics in terms of field strength and direction, particularly those with antiferromagnetic order, and a detailed comparison with Q1D theory, including the full details of the DM interaction, would provide a powerful test of the ideas described above, as could quantitative understanding of magnetic Raman scattering [72–75].

---

[*]bjpowell@gmail.com

[1] B. J. Powell and R. H. McKenzie, Rep. Prog. Phys. **74**, 056501 (2011).

[2] Y. Shimizu, K. Miyagawa, K. Kanoda, M. Maesato, and G. Saito, Phys. Rev. Lett. **91**, 107001 (2003).

[3] Y. Shimizu, T. Hiramatsu, M. Maesato, A. Otsuka, H. Yamochi, A. Ono, M. Itoh, M. Yoshida, M. Takigawa, Y. Yoshida, and G. Saito, Phys. Rev. Lett. **117**, 107203 (2016).

[4] T. Itou, A. Oyamada, S. Maegawa, M. Tamura, and R. Kato, Phys. Rev. B **77**, 104413 (2008).

[5] L. Balents, Nature (London) **464**, 199 (2010).

[6] R. Coldea, D. A. Tennant, K. Habicht, P. Smeibidl, C. Wolters, and Z. Tylczynski, Phys. Rev. Lett. **88**, 137203 (2002).

[7] R. Coldea, D. A. Tennant, A. M. Tsvelik, and Z. Tylczynski, Phys. Rev. Lett. **86**, 1335 (2001); R. Coldea, D. A. Tennant, and Z. Tylczynski, Phys. Rev. B **68**, 134424 (2003).

[8] H. Kino and H. Fukuyama, J. Phys. Soc. Jpn. **65**, 2158 (1996).

[9] R. H. McKenzie, Comments Condens. Matter Phys. **18**, 309 (1998).

[10] T. Koretsune and C. Hotta, Phys. Rev. B **89**, 045102 (2014).

[11] E. Scriven and B. J. Powell, Phys. Rev. B **80**, 205107 (2009).

[12] A. L. Khosla, A. C. Jacko, J. Merino, and B. J. Powell, Phys. Rev. B **95**, 115109 (2017).

[13] J. Merino, A. C. Jacko, A. L. Khosla, and B. J. Powell, arXiv:1703.0834.

[14] We use DIRACQ, J. G. Wright and B. S. Shastry, arXiv:1301.4494, to handle the bookkeeping.

[15] L. Cano-Cortés, A. Dolfen, J. Merino, J. Behler, B. Delley, K. Reuter, and E. Koch, Eur. Phys. J. B **56**, 173 (2007).

[16] L. Cano-Cortés, J. Merino, and S. Fratini, Phys. Rev. Lett. **105**, 036405 (2010).

[17] T. Mori, Bull. Chem. Soc. Jpn. **73**, 2243 (2000).

[18] E. P. Scriven and B. J. Powell, Phys. Rev. Lett. **109**, 097206 (2012).

[19] M. Kohno, O. A. Starykh, and L. Balents, Nat. Phys. **3**, 790 (2007).

[20] J. Merino, R. H. McKenzie, J. B. Marston, and C. H. Chung, J. Phys. Condens. Matter **11**, 2965 (1999); A. E. Trumper, Phys. Rev. B **60**, 2987 (1999).

[21] O. A. Starykh, H. Katsura, and L. Balents, Phys. Rev. B **82**, 014421 (2010).

[22] B. J. Powell and R. H. McKenzie, Phys. Rev. Lett. **98**, 027005 (2007).

[23] W. Zheng, J. O. Fjærestad, R. R. P. Singh, R. H. McKenzie, and R. Coldea, Phys. Rev. Lett. **96**, 057201 (2006).

[24] J. O. Fjærestad, W. Zheng, R. R. P. Singh, R. H. McKenzie, and R. Coldea, Phys. Rev. B **75**, 174447 (2007).

[25] Z. Weihong, R. H. McKenzie, and R. P. Singh, Phys. Rev. B **59**, 14367 (1999).

[26] T. Pardini and R. R. P. Singh, Phys. Rev. B **77**, 214433 (2008).

[27] A. Weichselbaum and S. R. White, Phys. Rev. B **84**, 245130 (2011).

[28] R. F. Bishop, P. H. Y. Li, D. J. J. Farnell, and C. E. Campbell, Phys. Rev. B **79**, 174405 (2009).

[29] O. A. Starykh and L. Balents, Phys. Rev. Lett. **98**, 077205 (2007).

[30] D. Heidarian, S. Sorella, and F. Becca, Phys. Rev. B **80**, 012404 (2009).

[31] M. Q. Weng, D. N. Sheng, Z. Y. Weng, and R. J. Bursill, Phys. Rev. B **74**, 012407 (2006).

[32] M. Bocquet, F. H. L. Essler, A. M. Tsvelik, and A. O. Gogolin, Phys. Rev. B **64**, 094425 (2001).

[33] J. Merino, M. Holt, and B. J. Powell, Phys. Rev. B **89**, 245112 (2014).

[34] D. F. Smith, S. M. De Soto, C. P. Slichter, J. A. Schlueter, A. M. Kini, and R. G. Daugherty, Phys. Rev. B **68**, 024512 (2003).

[35] D. F. Smith, C. P. Slichter, J. A. Schlueter, A. M. Kini, and R. G. Daugherty, Phys. Rev. Lett. **93**, 167002 (2004).

[36] F. Kagawa, Y. Kurosaki, K. Miyagawa, and K. Kanoda, Phys. Rev. B **78**, 184402 (2008).

[37] A. Antal, T. Fehér, B. Nàfràdi, L. Forró, and A. Jánossy, J. Phys. Soc. Jpn. **84**, 124704 (2015).

[38] S. M. Winter, K. Riedl, and R. Valentí, Phys. Rev. B **95**, 060404 (2017).

[39] We report our results in the Brillouin zone relevant before the unit cell is doubled by the pattern of DM vectors and neglect the bilayer structure of CuCN and AgCN as first principles calculations [38] suggest that the DM vector is not staggered in this direction.

[40] A. C. Jacko (private communication).

[41] T. Giamarchi, *Quantum Physics in One Dimension* (Clarendon Press, Oxford, 2004).

[42] S. Yamashita, Y. Nakazawa, M. Oguni, Y. Oshima, H. Nojiri, Y. Shimizu, K. Miyagawa, and K. Kanoda, Nat. Phys. **4**, 459 (2008).

[43] M. Yamashita, N. Nakata, Y. Kasahara, T. Sasaki, N. Yoneyama, N. Kobayashi, S. Fujimoto, T. Shibauchi, and Y. Matsuda, Nat. Phys. **5**, 44 (2009).

[44] E. Shimshoni, D. Rasch, P. Jung, A. V. Sologubenko, and A. Rosch, Phys. Rev. B **79**, 064406 (2009).

[45] Compare supplementary information for [43] with Fig. 2 of [44].

[46] I. Kézsmárki, Y. Shimizu, G. Mihály, Y. Tokura, K. Kanoda, and G. Saito, Phys. Rev. B **74**, 201101(R) (2006); S. Elsässer, D. Wu, M. Dressel, and J. A. Schlueter, Phys. Rev. B **86**, 155150 (2012).

[47] M. Dressel (private communication).

[48] W. Zheng, R. R. P. Singh, R. H. McKenzie, and R. Coldea, Phys. Rev. B **71**, 134422 (2005).

[49] S. Eggert, I. Affleck, and M. Takahashi, Phys. Rev. Lett. **73**, 332 (1994).

[50] E. Yusuf, B. J. Powell, and R. H. McKenzie, Phys. Rev. B **75**, 214515 (2007).

[51] B. J. Powell, E. Yusuf, and R. H. McKenzie, Phys. Rev. B **80**, 054505 (2009).

[52] S. S. Lee, P. A. Lee, and T. Senthil, Phys. Rev. Lett. **98**, 067006 (2007).

[53] Y. Qi and S. Sachdev, Phys. Rev. B **77**, 165112 (2008).

[54] Y. Qi, C. Xu, and S. Sachdev, Phys. Rev. Lett. **102**, 176401 (2009).

[55] G. Baskaran, Phys. Rev. Lett. **63**, 2524 (1989).

[56] J. Liu, J. Schmalian, and N. Trivedi, Phys. Rev. Lett. **94**, 127003 (2005).

[57] B. Kyung and A.-M. S. Tremblay, Phys. Rev. Lett. **97**, 046402 (2006).

[58] T. Grover, N. Trivedi, T. Senthil, and P. A. Lee, Phys. Rev. B **81**, 245121 (2010).

[59] V. Galitski and Y. B. Kim, Phys. Rev. Lett. **99**, 266403 (2007).

[60] H. Kawamura and S. Miyashita, J. Phys. Soc. Jpn. **53**, 4138 (1984).

[61] H. Li, R. T. Clay, and S. Mazumdar, J. Phys. Condens. Matter **22**, 272201 (2010).

[62] M. Dupont, S. Capponi, and N. Laflorencie, Phys. Rev. B **94**, 144409 (2016).

[63] M.-A. Vachon, G. Koutroulakis, V. F. Mitrović, O. Ma, J. B. Marston, A. P. Reyes, P. Kuhns, R. Coldea, and Z. Tylczynski, New J. Phys. **13**, 093029 (2011).

[64] Y. Tokiwa, T. Radu, R. Coldea, H. Wilhelm, Z. Tylczynski, and F. Steglich, Phys. Rev. B **73**, 134414 (2006).

[65] R. S. Manna, M. de Souza, A. Brühl, J. A. Schlueter, and M. Lang, Phys. Rev. Lett. **104**, 016403 (2010).

[66] M. Poirier, S. Parent, A. Côté, K. Miyagawa, K. Kanoda, and Y. Shimizu, Phys. Rev. B **85**, 134444 (2012).

[67] M. Poirier, M. de Lafontaine, K. Miyagawa, K. Kanoda, and Y. Shimizu, Phys. Rev. B **89**, 045138 (2014).

[68] Y. Shimizu, K. Miyagawa, K. Kanoda, M. Maesato, and G. Saito, Phys. Rev. B **73**, 140407(R) (2006).

[69] J. Merino, M. Dumm, N. Drichko, M. Dressel, and R. H. McKenzie, Phys. Rev. Lett. **100**, 086404 (2008).

[70] S. Milbradt, A. A. Bardin, C. J. S. Truncik, W. A. Huttema, A. C. Jacko, P. L. Burn, S.-C. Lo, B. J. Powell, and D. M. Broun, Phys. Rev. B **88**, 064501 (2013).

[71] B. J. Powell, J. Phys. Condens. Matter **18**, L575 (2006).

[72] Y. Nakamura, N. Yoneyama, T. Sasaki, T. Tohyama, A. Nakamura, and H. Kishida, J. Phys. Soc. Jpn. **83**, 074708 (2014).

[73] Y. Nakamura, T. Hiramatsu, Y. Yoshida, G. Saito, and H. Kishida, J. Phys. Soc. Jpn. **86**, 014710 (2017).

[74] N. Drichko, R. Hackl, and John A. Schlueter, Phys. Rev. B **92**, 161112(R) (2015).

[75] N. Hassan, S. Cunningham, M. Mourigal, E. I. Zhilyaeva, S. A. Torunova, R. N. Lyubovskaya, and N. Drichko, arXiv:1704.04482.